Performance Analysis of On-Board Vehicle Sensors on Positioning in GNSS Signal Blockage

Joong-hee HAN, Yong LEE, and Jay Hyoun KWON, Korea

Key words: Wheel Speed Sensor, Steering Angle Sensor, Extended Kalman Filter, Vehicle Positioning System

SUMMARY

The GNSS based positioning technique has been widely applied for the vehicle positioning in last two decades. In spite of its high accuracy and reliability in open area, the performance of the GNSS based positioning is significantly unstable in urban canyon. To solve this problem, it is necessary to integrate additional sensors. Recently, to improve driving safety and convenience, the vehicle is equipped with multi-sensors in order to operate ADAS. Therefore, the accuracy of vehicle positioning in urban canyon could be improved using several on-board vehicle sensors built in the vehicle. In this study, GNSS/on-board vehicle sensors integrated vehicle positioning algorithm is developed, and performance analysis is conducted during GNSS outages using real data. The integration strategy are proposed for the integration of the GNSS, wheel speed sensor, and steering angle sensor. The vehicle positioning algorithm on the basis of the kinematic vehicle model provides horizontal position, vehicle velocity, and yaw through an extended Kalman filter. The performance of the vehicle positioning algorithm is analyzed using the data from real test driving.

Performance Analysis of On-Board Vehicle Sensors on Positioning in GNSS Signal Blockage

Joong-hee HAN, Yong LEE, and Jay Hyoun KWON, Korea

1. INTRODUCTION

The GNSS-based positioning technique has been broadly applied for the automotive navigation system. Although it provides the navigation solution with high accuracy for a long time, it is unable to ensure the continuity and the reliability in an urban canyon. To overcome this kind of problem, new types of navigation systems which combine GNSS with dead-reckoning system based on a micro electro mechanical systems (MEMS) based inertial measurement unit (IMU) and various estimation techniques, were studied in the previous studies (Shin, 2005; Godha and Cannon, 2007; Zhou *et al*., 2010; Zhao, 2011; Quinchia *et al*., 2013). However, the accuracy and the reliability of dead-reckoning system based on the MEMS-IMU are significantly degraded due to large uncertainties in the MEMS-IMU output when GNSS signal is blocked for several minutes. Also, if MEM-IMU can provide the navigation solution to fulfill the requirement accuracy for the automotive navigation system, it is far too costly for use in the commercial navigation system.

Recently, advanced driver assistance system (ADAS) applications including anti-lock brake system, vehicle stability control system, and adaptive cruise control are being applied to the passenger car to improve safety and convenience in driving. Since numerous on-board vehicle sensors (e.g. steering angle sensor, wheel speed sensor, gravity sensor, radar, and camera) have been equipped to operate ADAS application, those sensors would be applied to compensate the limitations of the GNSS-based positioning technique. Especially, the integration of GNSS with both a steering angle sensor (SAS) and a wheel speed sensor (WSS) that are standard equipment in passenger car has been extensively studied to estimate reliable vehicle states for localization as well as vehicle dynamic control in the limited GNSS visibility environments. Despite that, additional research to analyze the performance of vehicle state estimation is necessary. It is because the performance could be largely dependent on the driving environment and the filter design.

In this study, a vehicle positioning algorithm that integrates GNSS with on-board vehicle sensors (wheel speed sensor and steering angle sensor) is developed to analyze the performance of on-board vehicle sensors on positioning in the environment of GNSS signal blockage. And then, the performance analysis of WSS/SAS integration during GNSS outages is conducted.

2. GNSS/ON-BOARD VEHICLE SENSOR INTEGRATION

2.1 Vehicle Motion and Mechanization Equation

The bicycle model is the one of the popular models to represent the motion of the ground vehicle. The bicycle model is classified into two models: the kinematic vehicle model which derives geometric relationship and the dynamic vehicle model which considers the lateral vehicle motion(Rajamani, 2006). While the kinematic vehicle model is suitable for the low-speed motion of the vehicle, the dynamic vehicle model is applied for high-speed and large wheel slip condition (Jo *et al*., 2012). Due to difficulties in acquiring parameters of the dynamic vehicle model such as front and rear slip angle, tire cornering stiffness, and angular speed of the wheels (Shin, 2005), the kinematic vehicle model is applied in this study.

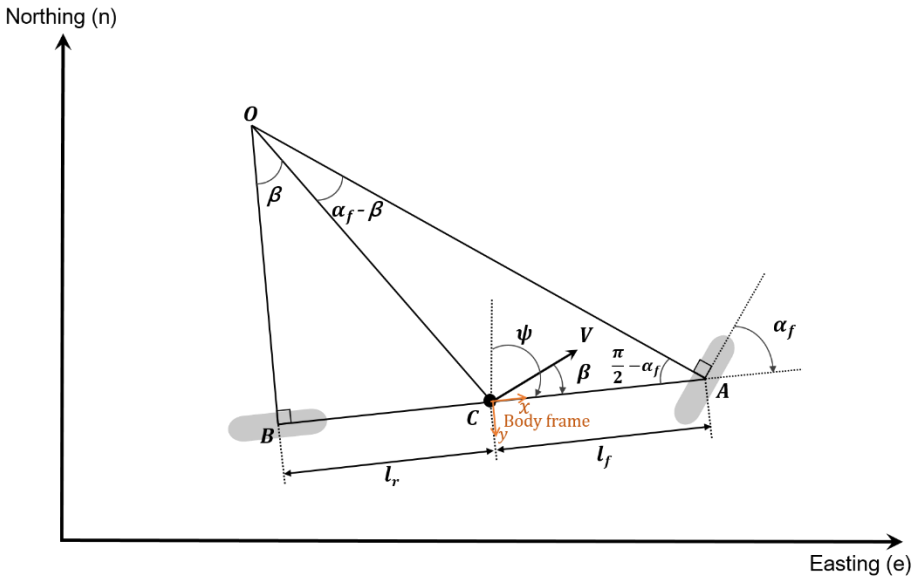

Figure 2.1 The kinematic vehicle model

Figure 2.1 shows the kinematic vehicle model. In the bicycle model, a pairs of left and right wheels are represented by a central wheel. In the figure, point A and B represent the center of the front and the rear wheels, respectively. The center of gravity of the vehicle is point C. The distances from C to point A and B are l_f and l_r. α_f describes the front wheel steering angle from steering angle sensor and steering ratio. The magnitude of velocity at point C is denoted by V. ψ is the yaw angle, and β is the vehicle slip angle. The equations of vehicle motion are shown as below:

$$\begin{bmatrix} \dot{n} \\ \dot{e} \end{bmatrix} = \begin{bmatrix} \cos(\psi+\beta) & -\sin(\psi+\beta) \\ \sin(\psi+\beta) & \cos(\psi+\beta) \end{bmatrix} \begin{bmatrix} v_x^b \\ v_y^b \end{bmatrix} \tag{2.1}$$

$$\dot{\psi} = \frac{V\cos(\beta)}{L}\tan(\alpha_f) \tag{2.2}$$

$$\beta = \tan^{-1}\left(\frac{l_r\tan(\alpha_f)}{L}\right) \tag{2.3}$$

where $\dot{n}$ and $\dot{e}$ are the north and east velocity in the navigation frame, respectively; $\dot{\psi}$ is the angular velocity of vehicle; $L = l_f + l_r$ is the wheelbase of vehicle; v_x^b and v_y^b are the body velocity computed from Equation (2.4).

$$\begin{bmatrix} v_x^b \\ v_y^b \end{bmatrix} = \begin{bmatrix} v_x^w \\ 0 \end{bmatrix} + \begin{bmatrix} 0 \\ -l_r \end{bmatrix}\dot{\psi}^w \tag{2.4}$$

The Longitudinal velocity v_x^w and the yaw rate $\dot{\psi}^w$ at the center of rear wheels are computed based on the rear wheel speed sensor measurement using following equations.

$$v_x^w = \frac{v_L^w + v_R^w}{2} \tag{2.5}$$

$$\dot{\psi}^w = \frac{v_L^w - v_R^w}{T_r} \tag{2.6}$$

where v_L^w and v_R^w are the rear left and rear right wheel speed, respectively; T_r is rear track width of vehicle.

2.2 GNSS/On-board Vehicle Sensor Integration

Figure 2.2 shows the GNSS/SAS/WSS integration strategy. The vehicle positioning algorithm is implemented based on an extended Kalman filter (EKF). Horizontal position, velocity, yaw, slip angle are computed using kinematic vehicle model at 50Hz when WSS and SAS measurements are available. The position measument of GNSS code based absolute positioning is integrated by a loosley coupled strategy at 1 Hz. The state vector of sensor error is composed of wheel speed sensor scale factor, and steering angle sensor scale factor.

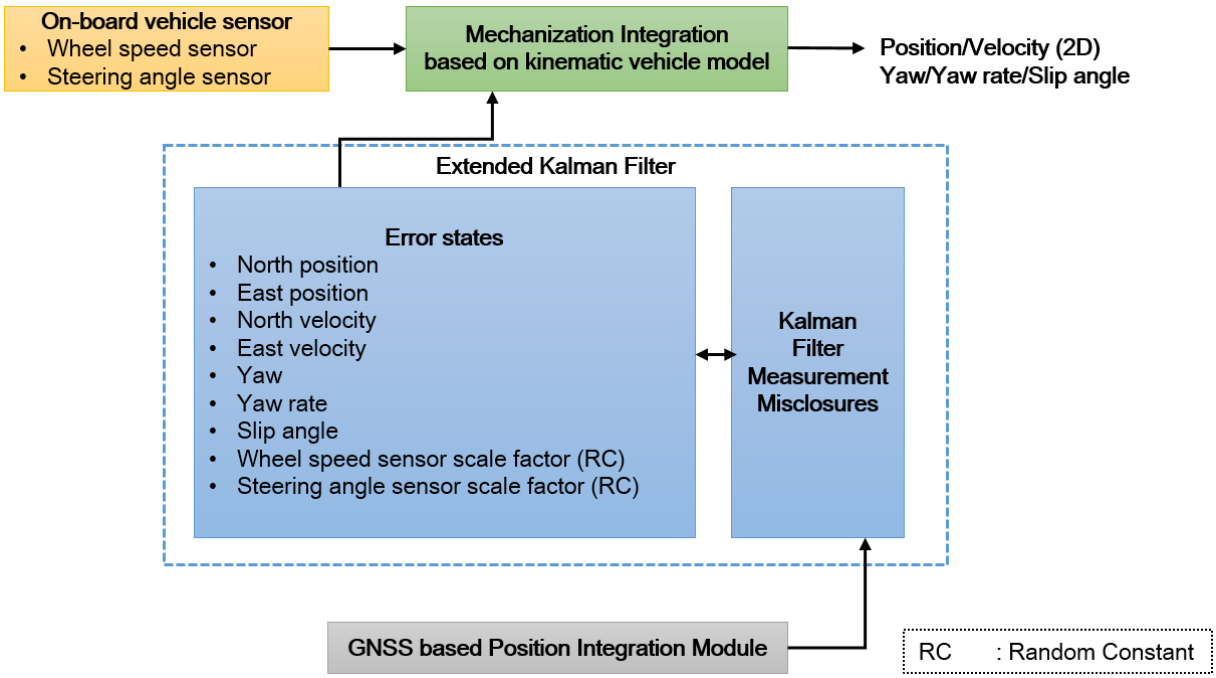

Figure 2.2 GNSS/SAS/WSS Integration Strategy

3. PERFORMANCE ANALYSIS

3.1 Test Descriptions

Test was conducted on November 9, 2015 in nearby Daegu Gyeonbuk Institute of Science and Technology (DGIST), which is suburban area. The test trajectory is shown in Figure 3.1. The total duration of test is approximately 32 minutes with frequent stops due to the traffic sign. The total distance traveled was about 11 km. The speed of the vehicle varies 0 ~ 65m/h.

The on-board vehicle sensor data were obtained from an in-vehicle network CAN without installation. The position information of GNSS code based absolute positioning were acquired by a NovAtel's DL-V3-GENERIC receiver. To evaluate the performance of the proposed algorithm, the reference data was generated by an Applanix's POS LV 520 system in post-mission.

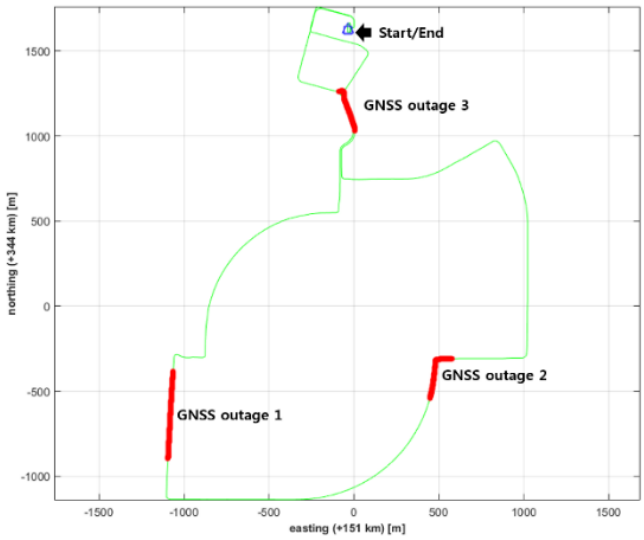

Figure 3.1 Test trajectory with simulating GNSS outage

To analyze the performance of on-board vehicle sensors on positioning during GNSS, three GNSS outages were simulated with a duration of 30s. The simulated GNSS outages are labelled by the red lines in Figure 3.1. The speed and ellipsoidal height from reference data associated with three simulated GNSS outages are shown in Figure 3.2.

In the case of GNSS outage 1, the vehicle is travelling along a straight path on a flat road. The vehicle in GNSS outage 2 is moved along a sharp corner path on sloping road. The case of GNSS outage 3 contains three speed bump on sloping road. There are relatively large change in the speed.

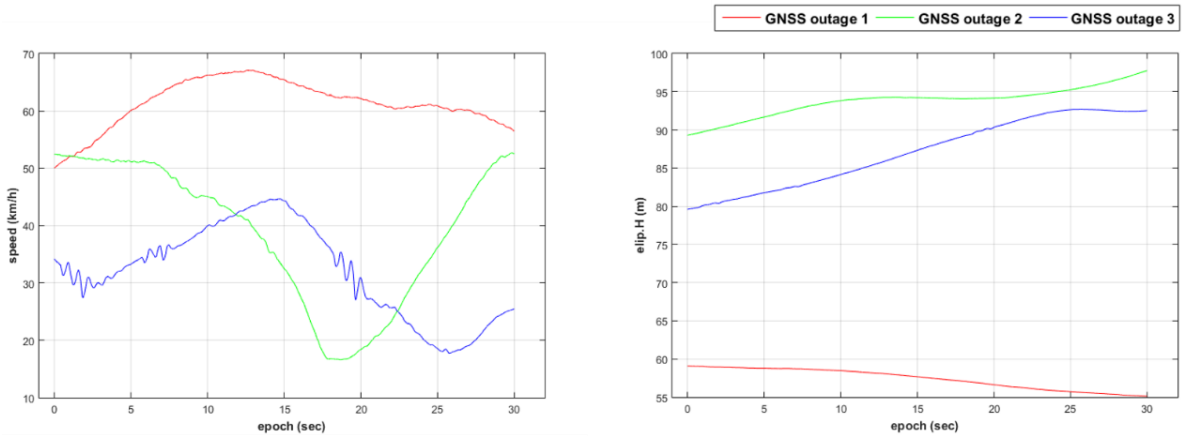

Figure 3.2 Speed and Eliposidal height of Vehicle in GNSS outages

3.2 Performance Analysis

In the performance analysis, we compared the horizontal position error of SAS/WSS integration on different vehicle dynamics during GNSS outages. The horizontal position of SAS/WSS integration with reference data for the three GNSS outages is presented in Figure 3.3. The statistics

of the horizontal position error are summarized in Table 3.1. In spite of travelling straight path, GNSS outage 1 presents the worst result, having a maximum horizontal error 49.66 m and a mean horizontal error of 20.74 m. In the case of GNSS outage 2, during the turns, the horizontal position error drastically increased owing to large uncertainty of yaw rate derived from on-board vehicle sensor. From the above results, it seems that the accuracy of position is drastically degraded when the vehicle travels on an abrupt turn in the road or at a very high speed.

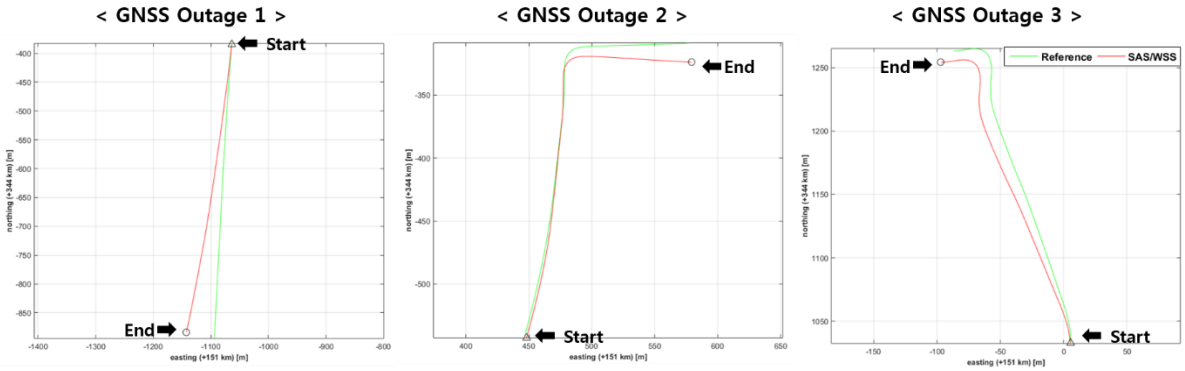

Figure 3.3 Horizontal Position during GNSS outages

Table 3.1 Maximum and mean horizontal position error during GNSS outages

Outage	Duration (sec)	Average Speed (km/h)	Horizontal Position Error	
			Mean (m)	Max (m)
1	**30**	**61**	**19.62**	**49.66**
2	**30**	**39**	**5.60**	**15.34**
3	**30**	**32**	**8.51**	**13.62**

In order to analyze the relationship between the vehicle speed and positon error, the vehicle velocity is derived by the measurement of wheel speed sensors using equation 2.4. And then, we compared the vehicle speed derived rear wheel speed sensor and the vehicle speed error with respect to reference data. As seen in Figure 3.4, the error of vehicle speed derived rear wheel speed sensor is generally increased along with magnitude of vehicle speed. Also, the magnitude of vehicle speed outlier is proportional to the magnitude of vehicle speed. It is seem that the result of GNSS outage 1 might be caused by wheel slipping and skidding due to whether uneven road or vehicle dynamic force. Therefore, we consider this is due to the better estimation of SAS/WSS integration which needs more analysis.

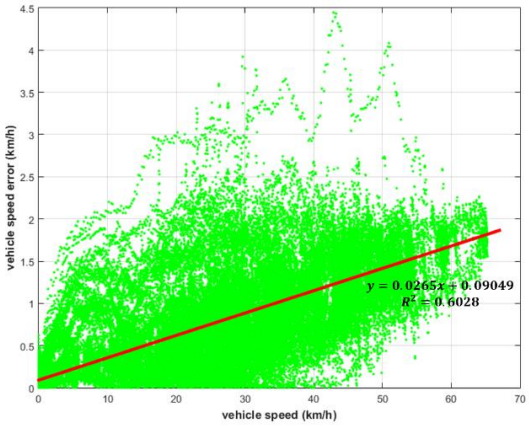

Figure 3.4 The error of vehicle speed derived by rear wheel speed sensor with vehicle speed

4. CONCLUSION

In this paper, we presented the development of GNSS and steering angle sensor, and wheel speed sensor integration algorithm for land vehicle. The algorithm is implemented in a loosely coupled mode through an extended Kalman filter. To analyze the performance of dead-reckoning algorithm based on steering angle sensor and wheel speed sensor, the sensor and reference data was acquired by real test driving. Three simulated GNSS outages were set considering the vehicle dynamic condition. The results of performance analysis that the accuracy of WSS/SAS integration is affected by vehicle dynamics such as abrupt turn and very high speed. Also, the uncertainty of vehicle speed sensor measurement is correlated with vehicle speed. In order to improve the proposed algorithm, we will conduct the additional performance analysis, filter tuning and additional sensor integration.

ACKNOWLEDGEMENT

This research was supported by Basic Science Research Program through the National Research Foundation of Korea(NRF) funded by the Ministry of Education(NRF-2015R1D1A1A01061319).

REFERENCES

Godha, S., and Cannon, M. E, (2007). *GPS/MEMS INS integrated system for navigation in urban areas*, GPS Solutions, 11(3), 193-203.

Jo, K., Chu, K., & Sunwoo, M, (2012). *Interacting multiple model filter-based sensor fusion of GPS with in-vehicle sensors for real-time vehicle positioning*, Intelligent Transportation Systems, IEEE Transactions on, 13(1), 329-343.

Quinchia, A. G., Falco, G., Falletti, E., Dovis, F., and Ferrer, C. (2013), *A comparison between different error modeling of MEMS applied to GPS/INS integrated systems*, Sensors, 13(8), 9549-9588.

Rajamani, R. (2006), *Vehicle Dynamics and Control*, Springer-Verlag, New York, USA.

Shin, E. (2005), *Estimation techniques for low-cost inertial navigation*, Ph.D. Thesis, Department of Geomatics Engineering, University of Calgary, Canada.
Zhao, Y. (2011), *GPS/IMU integrated system for land vehicle navigation based on MEMS*, Licentiate Thesis, Division of Geodesy and Geoinformatics, Royal Institute of Technology (KTH), Sweden.
Zhou, J., Edwan, E., Knedlik, S., & Loffeld, O. (2010), *Low-cost INS/GPS with nonlinear filtering methods*, In Information Fusion (FUSION), 2010 13th Conference on IEEE, 1-8.

CONTACTS

Ph. D Student, **Joong-hee Han**
University of Seoul
163 Seoulsiripdaero, Dongdaemun-gu,
Seoul
Republic of Korea
Tel. + 82-6490-5665
Fax + 82-6490-2884
Email: hjh0016@uos.ac.kr
Web site: gngl.uos.ac.kr

MS. Student, **Yong Lee**
University of Seoul
163 Seoulsiripdaero, Dongdaemun-gu,
Seoul
Republic of KOREA
Tel. + 82-6490-5665
Fax + 82-6490-2884
Email: acce00@uos.ac.kr
Web site: gngl.uos.ac.kr

Prof. Dr. **Jay Hyoun Kown**
University of Seoul
163 Seoulsiripdaero, Dongdaemun-gu,
Seoul
Republic of KOREA
Tel. + 82-6490-2890
Fax + 82-6490-2884
Email: jkwon@uos.ac.kr
Web site: gngl.uos.ac.kr